Published by Elsevier Science Inc.

ISSN 0735-1097/03/$30.00

doi:10.1016/S0735-1097(02)02867-X

Myocardial Perfusion and Viability by Positron Emission Tomography in Infants and Children With Coronary Abnormalities

Correlation With Echocardiography, Coronary Angiography, and Histopathology

Miguel Hernandez-Pampaloni, MD, PHD,* Vivekanand Allada, MD,† Michael C. Fishbein, MD,‡ Heinrich R. Schelbert, MD, PHD*

LOS ANGELES, CALIFORNIA

OBJECTIVES This study was designed to assess the feasibility and accuracy of positron emission tomography (PET) imaging in infants and children.

BACKGROUND Positron emission tomography is employed in adults for the evaluation of myocardial perfusion and the detection of myocardial viability.

METHODS Perfusion and metabolism findings on PET in infants and children with suspected coronary abnormalities (age 14 days to 12 years old, mean 3.3 ± 4.0 years) were correlated with findings on coronary angiography, echocardiography, and myocardial histopathology. The segmental myocardial uptake of the flow tracer ^{13}N-ammonia and of the glucose tracer ^{18}F-deoxyglucose (^{18}FDG) was graded on a five-point scale and compared with the angiographic perfusion score, with regional wall motion, and the presence of fibrosis.

RESULTS There was an agreement of $r = 0.72$ ($p < 0.05$) between regional myocardial perfusion and angiography. The correlation of histopathologic changes with normal, moderately, and severely reduced segmental ^{13}N-ammonia uptake was 87%, 60%, and 75%, respectively. Segmental myocardial ^{18}FDG uptake and histopathologic findings were concordant in 48 (79%) of 64 segments without fibrosis; absence of viability by perfusion and metabolism imaging correlated with the presence of fibrosis in 21 (84%) of 25 segments.

CONCLUSIONS The observed agreements between the findings on PET perfusion and metabolism imaging with those on coronary angiography, echocardiography, and histopathology support the utility and accuracy of PET for characterizing myocardial perfusion abnormalities and viability in pediatric patients. (J Am Coll Cardiol 2003;41:618–26) © 2003 by the American College of Cardiology Foundation

Coronary alterations, either congenital or acquired, with impairments of regional myocardial perfusion are an important cause of morbidity and mortality in infants and children (1–3). Identification of such coronary compromise, especially when associated with ischemia and potentially reversible contractile dysfunction, is clinically important (4,5). Regional myocardial perfusion defects following surgical repair of congenital heart disease can be detected with conventional radionuclide perfusion imaging (6,7). Visualization of flow defects in the small hearts of very young infants and children should also be possible with high spatial resolution positron emission tomography (PET). With PET, myocardial perfusion can be assessed with ^{13}N-ammonia and glucose utilization with ^{18}F-deoxyglucose (^{18}FDG). Use of PET is well established in adults for the detection of coronary artery disease and for the identification of myocardial viability (8–11). However, despite its high spatial resolution, PET has remained underutilized in the pediatric patient population. Therefore, the aims of this study were to examine in infants and children the relationship between myocardial perfusion by PET and coronary compromise and the accuracy of PET for the detection of viable or reversibly dysfunctional myocardium in comparison with findings on coronary angiography, echocardiography, and histopathology.

METHODS

Study design and population. Nine infants and children (age 14 days to 12 years; mean 3.3 ± 4.0 years, 5 female) with coronary abnormalities were studied (Table 1). Myocardial perfusion and glucose utilization were evaluated at rest with ^{13}N-ammonia and ^{18}FDG and PET and left ventricular (LV) function with two-dimensional echocardiography. All patients had coronary angiography. Histopathologic information was available either postmortem or after cardiac transplantation. In the seven children with prior surgical repair, the time from surgery to PET averaged 14 ± 2 months. In all nine children, the time from PET to cardiac transplantation or death was 45 ± 22 days; between PET and angiography, 6 ± 3 days; and between PET and echocardiography, 3 ± 4 days. The clinical indication for

From the Departments of *Molecular and Medical Pharmacology, †Pediatrics, and ‡Pathology, David Geffen School of Medicine at UCLA, University of California at Los Angeles, Los Angeles, California. Supported in part by the Director of the Office of Energy Research, Contract #DE-AC03-76-SF00012, OHER, Washington, DC; by Research Grant #HL 33177, NIH, Bethesda, MD; the Piansky Family Trust; and an AHA Clinician Scientist Award.

Manuscript received May 19, 2002; revised manuscript received August 2, 2002, accepted August 26, 2002.

Abbreviations and Acronyms

^{18}FDG	= ^{18}F-deoxyglucose
ANOVA	= analysis of variance
IV	= intravenous
LAD	= left anterior descending artery
LCX	= left circumflex coronary artery
LV	= left ventricular
PET	= positron emission tomography
RCA	= right coronary artery
ROI	= region of interest

the PET study was LV dysfunction. Seven patients had been hospitalized because of suspected myocardial ischemia (chest pain, ST-segment changes) and two with suspected acute myocardial infarction (new Q waves). The studies were performed in accordance with institutional guidelines, approval by the Institutional Review Board and with written parental consent.

As listed in Table 1, three of the patients had congenital coronary abnormalities (coronary-cameral fistula in the setting of pulmonary atresia and intact ventricular septum in two patients, and an intramural coronary artery coursing between the great arteries in the third patient). The remaining six patients had acquired coronary abnormalities, related in one to Kawasaki's disease with multiple coronary aneurysms and in five to postsurgical coronary abnormalities (three with coronary stenosis following the arterial switch operation in the neonatal period, one with a coronary obstruction following mitral valve repair and one with transplant vasculopathy with stenosis of the left anterior descending coronary artery [LAD]).

PET. Each patient was sedated with oral chloral hydrate (75 mg/kg), intravenous (IV) fentanyl (1 μg/kg/h) and midazolam (0.1 mg/kg/h), with supplemental doses as needed. Myocardial perfusion and metabolism were evaluated with standard whole body PET systems (ECAT 961 and ECAT 931, 6.5 mm full-width half-maximum, Siemens/CTI, Knoxville, Tennessee). Images were reconstructed with a Shepp-Logan filter with a cutoff frequency of 0.3 cycles/pixel, and reoriented into horizontal and vertical long-axis and short-axis views. Twenty-minute transmission images were recorded for correction of photon attenuation. Beginning 5 min after IV ^{13}N-ammonia (0.286 mCi/kg), static images were acquired for 20 min. Forty to 50 min later, ^{18}FDG (0.143 mCi/kg) was injected IV and acquisition of a 30-min static image began 40 min later. To stimulate myocardial glucose, and thus ^{18}FDG uptake, glucose (0.3 g/kg) was administered IV 1 h before the ^{18}FDG injection.

Image analysis. Using the standard 17-segment model, 16 regions of interest (ROI) were assigned to the LV myocardium, excluding, however, the apex because of apical thinning and the potential for misalignment. In each ROI, myocardial uptake of ^{13}N-ammonia and of ^{18}FDG was graded by two observers blinded to the clinical data on a 5-point scale: 4 = increased, 3 = normal, 2 = mildly reduced, 1 = moderately reduced, and 0 = severely reduced. Each segmental score was reached by consensus between the two readers. Myocardial segments with grade 3 ^{13}N-ammonia uptake were considered normal, regardless of ^{18}FDG uptake. Segments with concordantly reduced ^{13}N-ammonia and ^{18}FDG uptake scores were defined as having a blood flow-metabolism match. Segments with reduced ^{13}N-ammonia but normal, increased, or less severely reduced (by at least one grade) ^{18}FDG glucose uptake were classified as having a blood-flow metabolism mismatch (11). Inversely, segments with normal or increased ^{13}N-ammonia but reduced ^{18}FDG glucose uptake were classified as having a reverse blood-flow metabolism mismatch. The anterior wall, septum, and apex were considered to be subtended by the LAD, the lateral and posterior wall by the circumflex (LCX), and the inferior wall by the right coronary artery (RCA).

Echocardiography. Standard subcostal, apical, parasternal, and suprasternal notch views were obtained with an Acuson 128 Cardiac Imager (Mountain View, California) and recorded on standard VHS tape. Wall motion was analyzed by consensus of two observers unaware of other clinical findings using the same LV segmentation as applied to the PET images and a 4-point scale: 3 = normal, 2 = mild hypokinesis, 1 = severe hypokinesis, and 0 = akinesis/dyskinesis.

Coronary angiography. Standard selective coronary or aortic root angiography was performed (12). The angiograms were analyzed visually by consensus of two pediatric cardiologists unaware of the other diagnostic data, applying a 4-point composite angiographic perfusion score for coronary patency and collateral circulation: 3 = normal coronaries or good collateral flow, 2 = 50% to 70% coronary stenosis with poor collateral flow, 1 = ≥70% stenosis with poor collateral flow, and 0 = complete occlusion without collaterals (13,14).

Histopathology. Following formalin fixation, the LV was sliced perpendicular to its long axis into a basal, mid, and apical third. Each slice was subdivided further to yield six sections of the LV. Transmural 2- to 3-mm thick tissue samples, including the endocardium and epicardium, were taken to match each of the 16 LV segments as used for analysis of echocardiograpic and PET images. All tissue specimens were processed routinely. Histological sections were stained with hematoxylin and eosin and trichrome. Each tissue specimen was examined for evidence of coagulation necrosis and/or fibrosis. Based on the degree of wall thinning and the amount of residual viable myocardium observed by visual analysis, the following pathology grades were used: 0 = <25%, 1 = 25% to 50%, 2 = 50% to 75%, and 3 = >75% viable, normally appearing myocytes. Eighty-nine tissue specimens were available for analysis.

Statistical analysis. Mean values are given with standard deviations. For correlating perfusion and metabolism scores with histopathologic findings and angiographic scores, lin-

Table 1. Clinical and Imaging Data of the Patient Population

Patient No.	Diagnosis	Age at Surgery	Surgery	Coronary Angiography	Echo (Hypo-/Akinesis)	Age at PET	Weight at PET (kg)	^{13}N-ammonia PET (Hypoperfusion)	PET Metabolism	PET Mismatch Location
1	d-TGA	6 days	ASO	LAD occlusion	LV global	24 days	3.2	Anterior, septum, apex, inferior	Mismatch	Inferior
2	d-TGA	8 days	ASO	RCA stenosis	LV global	2.3 mon	4.1	Inferior, posterior	Mismatch	Posterior
3	PA/IVS	4 days	RV patch	Normal	Septum	5.1 mon	4.6	Anterior, septum	Match	None
4	d-TGA, VSD, s/p Coart repair, PAB	4 days	ASO	LAD occlusion, RCA stenosis	Septum, inferior	1.6 mon	4.9	Septum, inferior	Mismatch	Lateral
5	AS, Sub-AS MS	3 yrs	MVR	LCX stenosis	NA	3.3 yrs	8	Inferior	Mismatch	Inferior
6	Kawasaki's disease	—	—	No stenosis, coronary aneurysms	Normal	4.8 mon	6.5	Normal	Normal	None
7	HLHS	7 yrs	OHT	LAD stenosis	Normal	10.5 yrs	33.4	Normal	Match	None
8	PA/IVS	3 days	BTS	RCA, LAD stenosis, PDA from RV	Lateral	13 days	3.2	Septum, RV freewall	Mismatch	RV freewall
9	DILV, restrictive BVF	11 yrs	BVF resection, PAB	RCA with intramural occlusion	LV global + outflow chamber akinesis	12.4 yrs	36	Midseptum, mid and sup RV infarction	Match	None

AS = aortic stenosis; ASO = arterial switch operation; BTS = Blalock-Taussing shunt; BVF = bulboventricular foramen; DILV = double inlet left ventricle; d-TGA = d-transposition of the great arteries; HLHS = hypoplastic left heart syndrome; IVS = intact ventricular septum; LAD = left anterior descending artery; LCX = left circumflex artery; MVR = mitral valve replacement; NA = not available; OHT = orthotopic transplant; PA = pulmonary atresia; PAB = pulmonary artery banding; PDA = patent ductus arteriosus; RCA = right coronary artery; RV = right ventricle; VSD = ventricular septal defect.

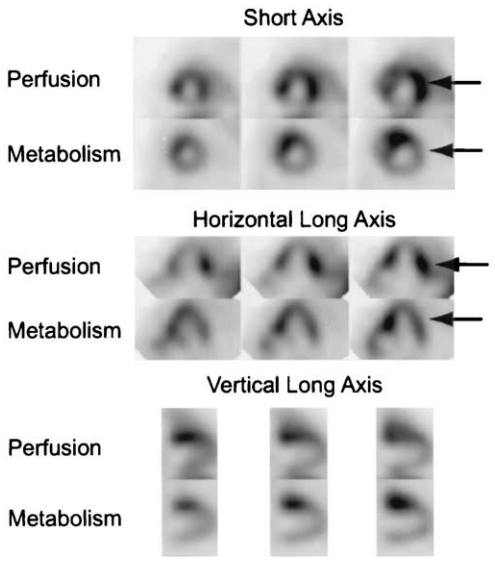

Figure 1. Myocardial ^{13}N-ammonia and ^{18}F-deoxyglucose images in Patient #4. Short and horizontal and vertical long axis slices are shown from **top to bottom**. As seen best on the short axis and the horizontal long axis slices, highlighted by the **arrows**, perfusion in the lateral wall is normal, whereas ^{18}F-deoxyglucose uptake is diminished ("reversed blood flow metabolism mismatch").

ear least square regressions were used. The agreement between modalities was evaluated with *kappa* statistics. Comparison of proportions between PET, echocardiography, and coronary angiography observations was made by chi-square analysis. Univariate one-way analysis of variance (ANOVA) was performed to characterize differences between segments classified according to the results of diagnostic methods. A p value of <0.05 was considered statistically significant.

RESULTS

Myocardial perfusion and glucose metabolism images in a 1.6-month-old child with d-transposition of the great arteries and a ventricular septal defect (Patient #4, Table 1) are shown in Figure 1. Perfusion in the lateral wall is normal, but ^{18}FDG uptake is reduced (arrows). Figure 2 depicts the histology in a tissue specimen removed from the lateral wall in the same patient.

Echocardiography and coronary angiography. The diagnostic quality of the echocardiographic studies was adequate in all but one patient (Patient #5) so that regional wall motion was analyzed in 128 segments in eight patients. Two patients had normal wall motion (Table 1). Wall motion was abnormal in 73 of the 128 segments. Table 2 correlates wall motion findings and angiographic scores. Although the correlation between the exact grades of perfusion and of wall motion failed to achieve statistical significance, allowing one grade disagreement resulted in a 67% agreement for all segments. Further, when segmental wall motion scores were averaged for each coronary artery territory, significant differences between coronary perfusion scores and severity of wall motion abnormalities became apparent. For example,

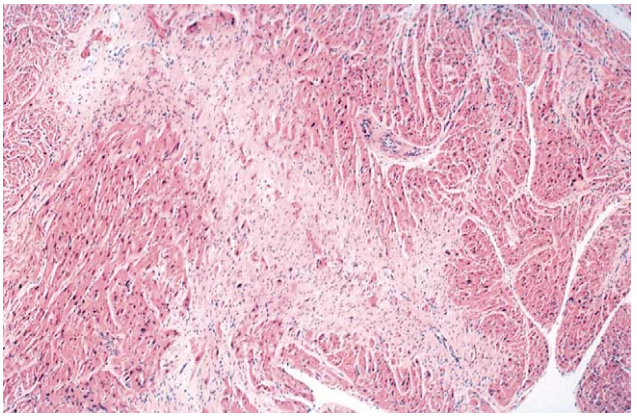

Figure 2. Tissue specimen obtained from the same patient shown in Fig. 1 from the lateral wall. Note the region of patchy fibrosis in the **center of the image**.

the angiographic score averaged 2.68 ± 0.39 in territories with normal wall motion, 1.17 ± 0.47 with mild hypokinesis, 0.94 ± 0.76 for territories with severe hypokinesis, and 1.4 ± 0.49 in territories with akinesis/dyskinesis ($p < 0.05$ by ANOVA all territories with abnormal vs. territories with normal wall motion).

Myocardial perfusion and coronary angiography. Of the 144 segments analyzed by PET and angiography, 92 revealed normal perfusion (Table 2). Of these, 81 segments (88%) were subtended by normal coronary arteries. Resting perfusion defects were present in 52 segments. Forty-nine (94%) of these had moderately to severely reduced perfusion scores on PET, and all were related to different degrees of coronary stenosis (angiographic perfusion scores from 0 to 2). The correlation between segmental angiographic and perfusion scores was statistically significant ($r = 0.72$; $p < 0.05$); further, one grade agreement between angiographic and perfusion scores (as defined previously) was found in 88% of segments (*kappa* value = 0.52). Accordingly, the composite angiographic scores correlated well with PET perfusion scores (mean angiographic score for segments with normal perfusion, 2.76 ± 0.35; mildly reduced, 1.4 ± 0.48; moderately reduced, 0.67 ± 0.36; and severely reduced 0; ANOVA, $p < 0.01$). When segments were grouped by coronary artery territory, the exact agreement for the LAD, LCX, and RCA was 62% (one-grade agreement 70%), 71% (98%), and 74% (100%), respectively.

Table 2. Myocardial Perfusion by ^{13}N-ammonia PET and Wall Motion Analysis by 2D-Echocardiography Versus Coronary Angiography

	No Coronary Stenosis	Coronary Stenosis	p Value
^{13}N-ammonia PET (n = 144)			
Perfusion normal	81	11	<0.01
Perfusion reduced	0	52	<0.01
2D-echocardiography (n = 128)			
Wall motion normal	36	19	<0.05
Wall motion abnormal	22	51	<0.05

PET = positron emission tomography.

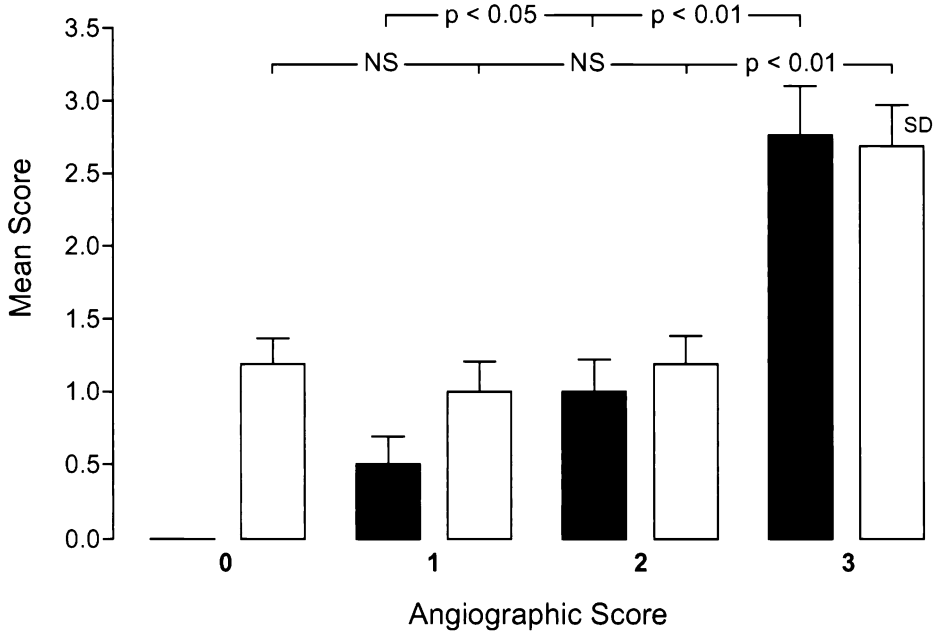

Figure 3. Comparison of segmental perfusion (positron emission tomography, **solid bars**, n = 144) and segmental wall motion scores (two-dimensional echocardiography, **open bars**, n = 128) with the angiographic scores. NS = not significant.

Myocardial perfusion and wall motion. The relationship between regional myocardial perfusion and wall motion was explored in the 128 myocardial segments analyzed by echocardiography. Wall motion was normal in 58 segments. In 55 (95%) of these, perfusion scores on PET were normal. Conversely, of the 70 segments with any degree of abnormal wall motion, 43 segments revealed hypoperfusion. For the 58 segments with normal wall motion perfusion, scores averaged 2.45 ± 0.34; for the 34 segments with mild hypokinesis, 1.18 ± 0.36; for the 19 segments with severe hypokinesis, 0.95 ± 0.41; and for the 17 with akinesis/dyskinesis, 1.24 ± 0.23. Figure 3 depicts perfusion and wall motion scores, relative to the angiographic scores. For segments with an angiographic score of 3 (i.e., normal coronary vessel), average scores for wall motion and perfusion were essentially normal. Wall motion scores were uniformly graded as severe hypokinesis for all abnormal angiographic perfusion scores (two or less), whereas relative perfusion scores progressively declined with increasingly severe angiographic scores.

Myocardial glucose utilization. Myocardial ^{18}FDG activity concentrations and myocardial perfusion were analyzed in 144 segments. Perfusion at rest was reduced in 43 segments. In 12 of such segments, ^{18}FDG uptake was maintained despite diminished perfusion, reflecting a flow metabolism mismatch; in the remaining 31 segments, ^{18}FDG uptake was decreased, representing a blood flow metabolism match. Importantly, 13 (68%) of the 19 myocardial segments with a more than one-grade disagreement between angiographic and perfusion scores (perfusion considered normal despite a ≥70% coronary stenosis, graded as 0 or 1) demonstrated normal uptake of ^{18}FDG.

Myocardial perfusion and histopathology. Of the 89 myocardial segments submitted to histopathology, only 25 segments revealed any degree of fibrosis. No coagulation necrosis was observed. Seven had extensive (<25% viable myocytes) and 18 had patchy, moderately severe fibrosis (25% to 75% viable myocytes). Of all 89 segments, 47 had a normal perfusion score. Forty-four of these segments were without evidence of fibrosis. The remaining 42 segments were associated with perfusion defects. Figure 4 depicts the relationship between the presence and absence of fibrosis and segmental perfusion. Among the 30 myocardial segments with scores of mildly to moderately reduced perfusion, only 12 presented with histological evidence of fibrosis. The remaining 18 segments were free of fibrosis. Furthermore, of the 12 segments with severely reduced perfusion, only 3 segments were without evidence of fibrosis. Finally, of the 47 segments with normal perfusion, only 4 segments revealed fibrosis.

Patterns of perfusion and metabolism. The histopathology findings were further correlated with the perfusion and ^{18}FDG metabolism scores (Table 3 and Fig. 5). Of the 64 segments with >75% viable myocytes (histopathology score 3), 49 segments (76%) were normal on PET, 12 segments (19%) revealed a match, and 3 (5%) a mismatch. In the 12 match segments, uptake of ^{13}N-ammonia and of ^{18}FDG was reduced by at least one grade. In the 25 remaining segments with <75% viable myocytes, a match pattern was found in 7 segments with extensive (<25% viable myocytes) and in 7 segments with moderate fibrosis (25% to 75%). Conversely, a mismatch pattern was noted in six segments with moderately patchy fibrosis and a reverse mismatch in six segments of the posterolateral wall.

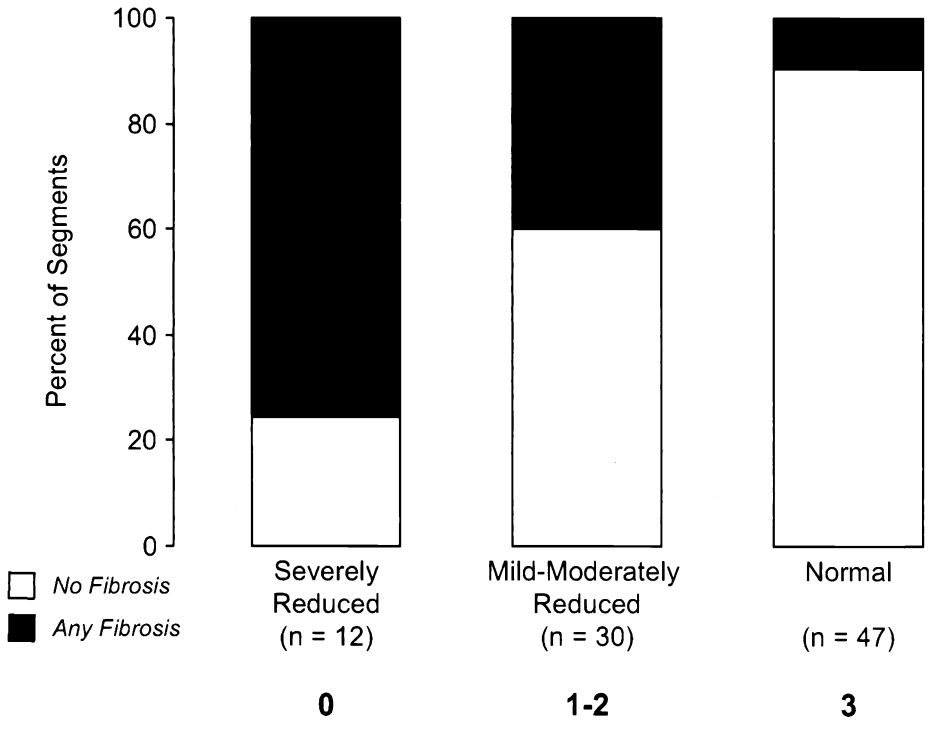

Figure 4. Comparison of segmental perfusion scores to findings on histopathology. Segments with grade 3 perfusion defects (severely reduced) to segments with normal perfusion are shown from **left to right**. For each **bar**, the **open area** depicts the percent of segments without fibrosis, and the **solid area** depicts the percent with any degree of fibrosis on histopathology.

Perfusion, glucose uptake, wall motion, angiography, and histopathology. The overall correlation between histopathology scores, the ^{18}FDG, the ^{13}N-ammonia uptake, and the wall motion scores is illustrated in Figure 6. Mean perfusion score progressively declines from segments without fibrosis to segments with extensive fibrosis; this decline becomes statistically significant between segments with grade 2 and with grade 1 histopathology scores ($p < 0.05$). Average ^{18}FDG uptake scores were reduced in segments with patchy fibrosis (25% to 75% viable myocytes) relative to segments without evidence of fibrosis. Further, average ^{18}FDG uptake was depressed most severely in segments with extensive fibrosis.

DISCUSSION

Noninvasive approaches have been used for the identification of myocardial perfusion abnormalities in children with congenital heart disease (15,16). High spatial resolution imaging with PET has, however, remained underutilized in pediatric patients (17). To our knowledge, this is the first study to compare in infants and children findings on myocardial perfusion and metabolism with PET to findings on coronary angiography and histopathology. In adults, identification of regional myocardial perfusion abnormalities and of myocardial viability by PET has been found clinically useful, as they contain predictive information on the potential for improvement in regional and global LV function after revascularization (10,11). Although no such outcome measures were available in the current study, perfusion defects as identified by ^{13}N-ammonia and PET were found to correlate with angiographic scores. Further, there was a good correlation between segmental perfusion and wall motion, although the severity of the segmental wall motion abnormality did not correlate directly with the severity of the segmental perfusion deficit. Segmental perfusion defects, however, correlated inversely with the degree of myocardial fibrosis on histopathology. Finally, perfusion metabolism mismatches as indices of myocardial viability were present most often in segments with moderately to severely reduced perfusion and intermediate degrees of fibrosis (25% to 75%).

Table 3. Tissue Characterization by PET versus Histopathology

Fibrosis	Normal or Mismatch	Match	p Value
Absent	52	12	<0.01
Present	6	19	<0.05

PET = positron emission tomography.

Segmental myocardial perfusion. Normal segmental perfusion was most frequently associated with angiographic scores of normal or good collateral blood flow. Most segments with reduced perfusion were subtended by coronary vessels with scores reflecting stenosis and limited collateral blood flow. However, 18% of segments subtended by abnormal coronary arteries (11/62) demonstrated normal perfusion. This disparity was observed in one patient (Patient #8) with an abnormal origin of the posterior descending coronary artery from the right ventricle and a second

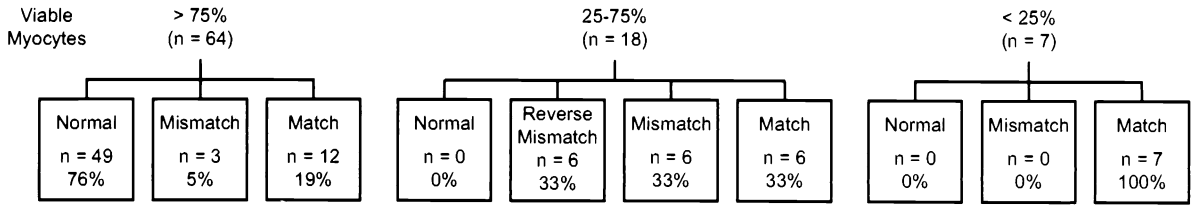

Figure 5. Correlation between the segmental amounts (in percent) of viable or normal myocytes and the corresponding blood flow metabolism patterns on positron emission tomography.

patient (Patient #4) with an occluded LAD coronary artery but with well developed collaterals to the anterior wall. In the first patient, elevated right ventricular pressures may have resulted in an adequate coronary driving pressure so that myocardial perfusion at rest was essentially normal. Had pharmacologic stress testing been performed, it might have uncovered coronary compromise (9,18). Misalignments of myocardial segments as identified on the PET images and as designated by coronary angiography may also account for some of the observed disparities. Such misalignment could further explain disparities between segmental perfusion and wall motion. Thus, wall motion was abnormal in 26 of the segments with normal perfusion. Seven normally perfused segments with reduced wall motion were subtended by coronary vessels with abnormal scores; again, these segments would probably have revealed, flow defects on pharmacologic stress testing.

Segmental perfusion defects were correlated with abnormal angiographic scores. Although perfusion was evaluated only at rest and would be expected to be normal in some segments supplied by abnormal coronary arteries, in 19 of 38 hypoperfused segments available for histopathologic correlation, various degrees of tissue fibrosis were noted. It is thus likely that resting myocardial perfusion was reduced as a function of the fractional amount of tissue fibrosis (19,20). In the remaining 72% of segments without histopathologic evidence of fibrosis, an impairment in wall motion and systolic thickening may have led to a partial volume related underestimation of regional myocardial perfusion. In fact, 15 (71%) of the segments with reduced perfusion but without fibrosis exhibited wall motion abnormalities.

Myocardial blood flow and metabolism. Coronary angiography provides excellent detail of the coronary anatomy, but little if any information on myocardial viability (21). Myocardial perfusion as assessed with ^{13}N-ammonia and

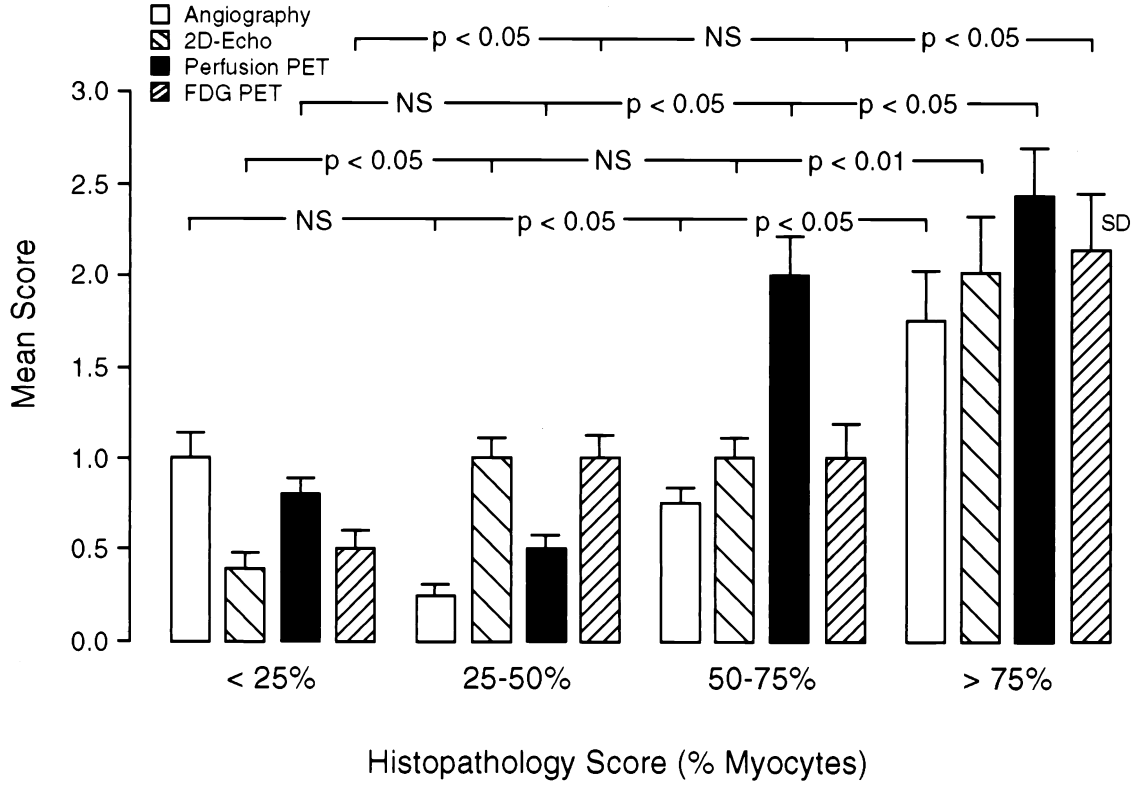

Figure 6. Comparisons of the mean angiographic, wall motion by echocardiography (2D-Echo), perfusion on positron emission tomography (Perfusion PET), and metabolism by ^{18}F-deoxyglucose on positron emission tomography (FDG PET) scores and the histopathologic grades.

PET can provide important information on the potential reversibility of regional myocardial dysfunction. Perfusion alone offered information on the presence or absence of myocardial viability. For example, myocardial segments with normal or, conversely, with severely reduced ^{13}N-ammonia uptake were strongly correlated with the absence or presence of tissue fibrosis, respectively. However, this correlation was weaker for segments with moderately reduced perfusion. In most of these segments (42 of 45), hypoperfusion was associated with abnormal wall motion. On histopathology, however, some segments revealed tissue fibrosis, whereas others did not. Thus, moderate reductions in perfusion appeared to discriminate insufficiently between reversible and irreversible regional myocardial dysfunction.

In such segments, ^{18}FDG may aid to identify myocardial viability. ^{18}F-deoxyglucose-PET revealed metabolic abnormalities in most segments with perfusion defects. Importantly, a mismatch pattern was found in four patients with severe coronary stenoses and wall motion abnormalities. As depicted in Figure 6, ^{18}FDG uptake correlated with the amount of fibrosis, indicating that glucose metabolism is markedly reduced in infarcted regions. Conversely, preserved myocardial metabolic activity in the entire LV indicates the absence of any significant coronary stenosis. In two children, myocardial ^{18}FDG was normal. Neither of these patients had evidence of any coronary stenosis or occlusion. Interestingly, six segments demonstrated a reverse mismatch with preserved myocardial perfusion but reduced metabolic activity. According to findings in post-thrombolysis patients (22), this pattern likely reflects myocardial viability.

Study limitations. A limitation to all nuclear imaging studies in infants and children is the lack of an age-specific database of normal findings. Ethical reasons preclude establishment of such normal databases in healthy infants and children. Therefore, prospective studies in a larger pediatric patient population would be needed for determining the significance of perfusion-metabolism patterns. However, it seems reasonable to assume that contractile function is likely to recover in dysfunctional myocardium with little to no fibrosis as compared with segments with >40% fibrosis that are unlikely to improve wall motion and, thus, would be considered "nonviable" or "irreversibly dysfunctional" (19,20). Normal variations in tracer uptake or transient postoperative metabolic changes without flow-limiting stenoses may have been related to mild hypoperfusion in some areas unrelated to coronary lesions and perhaps attributable to stunning (23). Further, the degree of fibrosis was not quantitated but estimated through visual analysis. In addition, it was not possible to precisely localize image segments.

Finally, three patients had been diagnosed with cyanotic heart disease, raising the possibility of a hypoxia-related effect on myocardial ^{18}FDG uptake. However, because of compensatory erythrocytosis, normal arterial O_2 concentrations, and a normal cardiac output, tissue hypoxia was unlikely to be present in these children.

Clinical implications. The correlation between angiographic and perfusion abnormalities indicates a potentially important role of high resolution PET for noninvasively identifying coronary abnormalities in pediatric patients. It may be considered a valid screening tool as well as an important adjunct to invasive angiography in selected populations. Our study demonstrates for the first time in a pediatric population that PET perfusion-metabolism imaging can provide important information on tissue viability. Positron emission tomography distinguished regions with marked tissue fibrosis from myocardium free of fibrosis. Because myocardial viability reflects potentially reversible regional and global LV dysfunction (8,10,11,20), PET imaging may provide clinically important information in pediatric patients, especially when surgical correction of coronary abnormalities is possible.

Acknowledgments

The authors thank Ron Sumida and his staff for assisting in the PET studies, N. Satyamurthy and his staff for providing the radiotracers, and Luke Deltredici and Akyaa Nickelson for the artwork.

Reprint requests and correspondence: Dr. Heinrich R. Schelbert, Department of Molecular and Medical Pharmacology, 23-120 CHS, Box 173517, Los Angeles, California 90095-6948. E-mail: hschelbert@mednet.ucla.edu.

REFERENCES

1. Bonnet D, Bonhoeffer P, Piechaud JF, et al. Long-term fate of the coronary arteries after the arterial switch operation in newborns with transposition of the great arteries. Heart 1996;76:274–9.
2. Day RW, Laks H, Drinkwater DC. The influence of coronary anatomy on the arterial switch operation in neonates. J Thorac Cardiovasc Surg 1992;104:706–12.
3. Tsuda E, Imakita M, Yagihara T, et al. Late death after arterial switch operation for transposition of the great arteries. Am Heart J 1992;124:1551–7.
4. Hausdorf G, Kampmann C, Schneider M. Coronary angioplasty for coronary stenosis after the arterial switch procedure. Am J Cardiol 1995;76:621–3.
5. Mavroudis C, Backer CL, Muster AJ, et al. Expanding indications for pediatric coronary artery bypass. J Thorac Cardiovasc Surg 1996;111:181–9.
6. Hayes AM, Baker EJ, Kakadeker A, et al. Influence of anatomic correction for transposition of the great arteries on myocardial perfusion: radionuclide imaging with technetium-99m 2-methoxy isobutyl isonitrile. J Am Coll Cardiol 1994;24:769–77.
7. Vogel M, Smallhorn JF, Gilday D, et al. Assessment of myocardial perfusion in patients after the arterial switch operation. J Nucl Med 1991;32:237–41.
8. Di Carli MF, Davidson M, Little R, et al. Value of metabolic imaging with positron emission tomography for evaluating prognosis in patients with coronary artery disease and left ventricular dysfunction. Am J Cardiol 1994;73:527–33.
9. Go RT, Marwick TH, MacIntyre WJ, et al. A prospective comparison of rubidium-82 PET and thallium-201 SPECT myocardial perfusion imaging utilizing a single dipyridamole stress in the diagnosis of coronary artery disease. J Nucl Med 1990;31:1899–905.
10. Marwick TH, Nemec JJ, Lafont A, et al. Prediction by postexercise fluoro-18 deoxyglucose positron emission tomography of improvement in exercise capacity after revascularization. Am J Cardiol 1992;69:854–9.

11. Tillisch J, Brunken R, Marshall R, et al. Reversibility of cardiac wall-motion abnormalities predicted by positron tomography. N Engl J Med 1986;314:884–8.
12. Takahashi M, Schieber RA, Wishner SH, et al. Selective coronary arteriography in infants and children. Circulation 1983;68: 1021–8.
13. Rentrop KP, Thornton JC, Feit F, Van Buskirk M. Determinants and protective potential of coronary arterial collaterals as assessed by an angioplasty model. Am J Cardiol 1988;61:677–84.
14. Robbins SL, Rodriguez FL, Wragg AL, Fish SJ. Problems in the quantitation of coronary arteriosclerosis. Am J Cardiol 1966;18: 153–9.
15. Bonhoeffer P, Bonnet D, Piechaud JF, et al. Coronary artery obstruction after the arterial switch operation for transposition of the great arteries in newborns. J Am Coll Cardiol 1997;29:202–6.
16. Weindling SN, Wernovsky G, Colan SD, et al. Myocardial perfusion, function and exercise tolerance after the arterial switch operation. J Am Coll Cardiol 1994;23:424–33.
17. Rickers C, Sasse K, Buchert R, et al. Myocardial viability assessed by positron emission tomography in infants and children after the arterial switch operation and suspected infarction. J Am Coll Cardiol 2000; 36:1676–83.
18. Yates RW, Marsden PK, Badawi RD, et al. Evaluation of myocardial perfusion using positron emission tomography in infants following a neonatal arterial switch operation. Pediatr Cardiol 2000;21:111–8.
19. Depre C, Vanoverschelde JL, Melin JA, et al. Structural and metabolic correlates of the reversibility of chronic left ventricular ischemic dysfunction in humans. Am J Physiol 1995;268:H1265–75.
20. Maes A, Flameng W, Nuyts J, et al. Histological alterations in chronically hypoperfused myocardium. Correlation with PET findings. Circulation 1994;90:735–45.
21. Formanek A, Nath PH, Zollikofer C, et al. Selective coronary arteriography in children. Circulation 1980;61:84–95.
22. Mesotten L, Maes A, Herregods MC, et al. PET "reversed mismatch pattern" early after acute myocardial infarction: follow-up of flow, metabolism and function. Eur J Nucl Med 2001;28:466–71.
23. Vanoverschelde JL, Wijns W, Depre C, et al. Mechanisms of chronic regional postischemic dysfunction in humans. New insights from the study of noninfarcted collateral-dependent myocardium. Circulation 1993;87:1513–23.